

THE ANALYSIS OF UNSTEADY FIELDS SHIELDING EFFICIENCY USING DOUBLE LAYERED SHEETS

Petre-MARIAN NICOLAE, Eleonor STOENESCU, Marius VOINEA

*University of Craiova, Faculty of Electrotechnics
pnicolae@elth.ucv.ro, estoenscu@elth.ucv.ro, mvoinea@elth.ucv.ro*

Abstract - The results of experimental tests emphasized the shielding efficiency when one uses sheets of *CuE* (electrolytic copper) and respectively of *steel* during the impact with the electromagnetic radiation. The variations of the wave impedance and of the penetration depth are analyzed for these materials with respect to the frequency range of 1...120 kHz.

The advantages of shielding with double layered sheets is deduced based on calculations concerning the behavior of the plane wave at the impact with the *steel* sheet and respectively with the *CuE* sheet.

Keywords: *shielding, unsteady fields*

1. INTRODUCTION

The reducing of radiated disturbances is performed using *electromagnetic shielding*. These are media that realize a separation between two distinct regions, one including the disturbances source and the other including the protected space. Inside the protected region the electromagnetic field strength is considerably reduced with respect to its counterpart from the unshielded domain.

Unlike the quasi-stationary alternative magnetic fields where only a reaction magnetic field occurs, in this case a reaction electric field is present. The shield becomes emitter and will transmit electromagnetic waves as described below.

The solenoidal electric field E^I of the incident electromagnetic wave generates currents in the shield's conducting walls according to the relation $J = \sigma E^I$, which at their turn generate a reaction magnetic field H^R . This last field generates, through induction, a solenoidal electric field E^R which, along with H^R forms the reflected electromagnetic wave. This mechanism is also valid for the quasi-steady regime. The solenoidal electric fields are so weak there that, in the non-conducting media, cannot produce displacing current which might have a significant contribution to the magnetic currents H_e and H^R caused by the conduction currents [1], [2].

In steady regimes, the field from the external space is formed by the superposition of the incident wave and of the secondary reflected wave, $E = E^I + E^R = 0$ respectively $E^I = -E^R$ [1], [3].

2. CONSIDERATIONS ON THE PLANE WAVE PROPAGATIONS

In a medium with the electric conductivity σ , the magnetic permeability μ and the permittivity ε , the equations of the plane electromagnetic wave propagation (similar to the telegraphers' equations) can be written under 2 forms [4]:

- The quantities near the source, with respect to the remote quantities [3]:

$$\underline{E}_1 = \underline{E}_2 \cosh kl + \underline{Z}_w \underline{H}_2 \sinh kl \quad (1)$$

$$\underline{H}_1 = \underline{H}_2 \cosh kl + \frac{\underline{E}_2}{\underline{Z}_w} \sinh kl \quad (2)$$

- The remote quantities, with respect to the quantities near the source:

$$\underline{E}_2 = \underline{E}_1 \cosh kl - \underline{Z}_w \underline{H}_1 \sinh kl \quad (3)$$

$$\underline{H}_2 = \underline{H}_1 \cosh kl - \frac{\underline{E}_1}{\underline{Z}_w} \sinh kl \quad (4)$$

With respect to the material properties the following properties may be mentioned [3], [4]:

- In metals: $\varepsilon = 0$; $\mu = \mu_0 \mu_r$; $\sigma \neq 0$.

The propagation constant:

$$k = \sqrt{j\omega\sigma\mu} = \frac{1+j}{\delta}; \quad \delta = \sqrt{\frac{2}{\omega\mu\sigma}} \quad (5)$$

The wave impedance $\underline{Z}_w = \sqrt{\frac{j\omega\mu}{\sigma}}$ (6)

- In air $\varepsilon = \varepsilon_0$; $\mu = \mu_0$; $\sigma = 0$.

The propagation constant:

$$k = j\omega\sqrt{\mu_0\varepsilon_0} \quad (7)$$

The wave impedance

$$\underline{Z}_0 = \sqrt{\frac{\mu_0}{\varepsilon_0}} = 377 \Omega \quad (8)$$

For the analysis and simulation of the penetration depth

(Fig.1) and respectively of the wave impedance (Fig.2) for *CuE* and *steel*, MATHAD programs were elaborated.

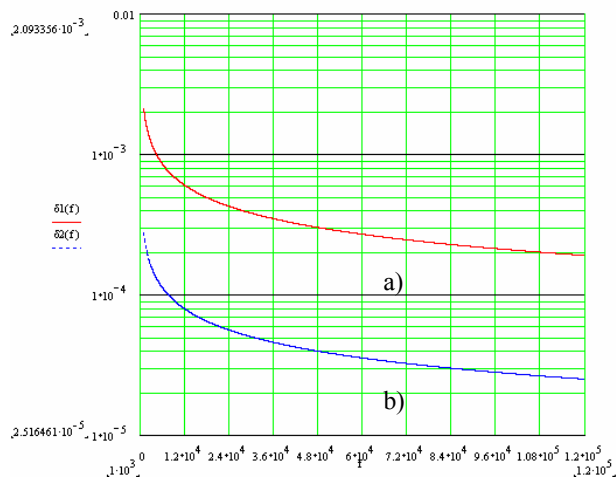


Figure 1: Depth penetration variation for *CuE* and *steel*

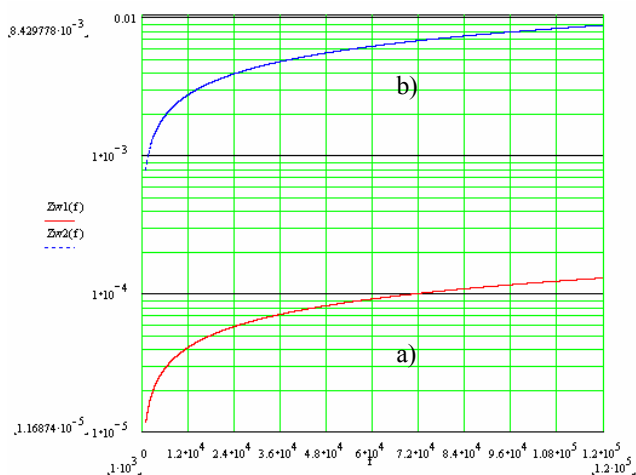


Figure 2: Wave impedance variation for *CuE* and *steel*

Fig. 1a emphasizes the variation of the depth penetration with respect to frequency when the plane wave penetrates a medium of *CuE* and fig. 1b depicts the variation of the depth penetration with respect to frequency when the plane wave gets out from a *steel* half-space.

Fig. 2a emphasizes the variation of the wave impedance with respect to frequency when the plane wave penetrates a medium of *CuE* and fig. 2b depicts the variation of the wave impedance with respect to frequency when the plane wave gets out from a *steel* half-space.

One used a frequency range of 1...120 kHz and a logarithmic scale was used along the *y* axis.

After the analysis of the depth penetration variation and of the wave impedance with respect to frequency one could

notice that the wave impedance is direct proportional to the frequency and that the depth penetration is inverse proportional to the frequency (the skin effect).

3. WAVE CROSSING FROM AIR TO THE CONDUCTING METAL

At the normal impact of the electromagnetic wave with a conducting half-space, bounded by a plane surface, a reaction is produced in the contact region (metal-air). This reaction can be quantified considering that the vectors \underline{E} and \underline{H} are tangent to the separation surface air-metal and consequently the tangential components of the electric and magnetic field are preserved. To this rule well known in Electrical Engineering one can add the following observations of phenomenological nature [5]: The incident wave is not found within the metal without modification and therefore one must accept a reflection process at the metal surface that alters in air the incident wave, in the impact zone. The reflected wave propagates in a sense opposite to the incident wave propagation sense [3].

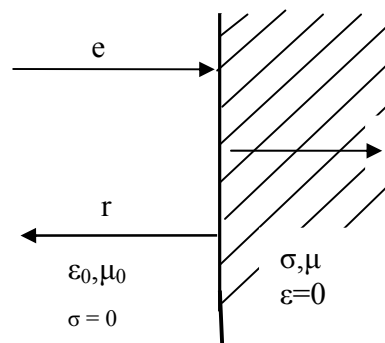


Figure 3: Metal penetration by a plane wave

The equations that describe the mentioned process are:

a) the phase equations

$$\underline{E}_e + \underline{E}_r = \underline{E}_i \quad (9)$$

$$\underline{H}_e + \underline{H}_r = \underline{H}_i \quad (10)$$

b) the relation for the propagation sense

$$\underline{H}_r = -\frac{\underline{E}_r}{\underline{Z}_0} \quad (11)$$

The equation (12) can be written under the form:

$$\frac{\underline{E}_e}{\underline{Z}_0} - \frac{\underline{E}_r}{\underline{Z}_0} = \frac{\underline{E}_i}{\underline{Z}_w}, \quad (12)$$

Here, if \underline{E}_r is substituted by its expression from (11) one gets:

$$\underline{E}_i = \frac{2\underline{Z}_w}{\underline{Z}_0 + \underline{Z}_w} \underline{E}_e = \underline{F}_1 \underline{E}_e, \quad (13)$$

where the expression:

$$\underline{F}_1 = \frac{2\underline{Z}_w}{\underline{Z}_0 + \underline{Z}_w} \quad (14)$$

represents the *refraction factor* and quantifies the electric field in the conducting half-space. In the equation (11) one knows \underline{E}_i from the equation (15) and so one can determine the reflected electric field:

$$\underline{E}_r = \frac{\underline{Z}_w - \underline{Z}_0}{\underline{Z}_w + \underline{Z}_0} \underline{E}_e = \underline{R}_1 \underline{E}_e \quad (15)$$

where the expression:

$$\underline{R}_1 = \frac{\underline{Z}_w - \underline{Z}_0}{\underline{Z}_w + \underline{Z}_0} \quad (16)$$

represents the *reflection factor* and quantifies the electric field reflected by the conducting metal surface. The relation between the refraction and reflection factors is [3]:

$$\underline{F}_1 = 1 + \underline{R}_1 \quad (17)$$

For the magnetic field quantification, considering (9) and (10), one uses the relations:

- in exterior, far away from the metallic surface:

$$\underline{H}_e = \frac{\underline{E}_e}{\underline{Z}_0} \quad (18)$$

- the reflected magnetic field:

$$\underline{H}_r = -\frac{\underline{E}_r}{\underline{Z}_0} \quad (19)$$

- the magnetic field transmitted at the boundary toward the metal inside:

$$\underline{H}_i = \frac{\underline{E}_i}{\underline{Z}_w} \quad (20)$$

A series of calculations were made in order to describe the electromagnetic state in the air and in the CuE metal at the impact with the plane electromagnetic wave [3].

- a) The reflection factor:

$$\underline{R}_1 = \frac{\underline{Z}_w / \underline{Z}_0 - 1}{\underline{Z}_w / \underline{Z}_0 + 1} = \frac{1,169 \cdot 10^{-4} e^{j\pi/4} / 377 - 1}{1,169 \cdot 10^{-4} e^{j\pi/4} / 377 + 1} \approx -1; \quad (21)$$

- b) The reflected electric field:

$$\underline{E}_r = \underline{E}_e \underline{R}_1 = -\underline{E}_e \quad (22)$$

- c) The electric field transmitted in metal, at the boundary:

$$\underline{E}_i = \underline{F}_1 \underline{E}_e = (1 + \underline{R}_1) \underline{E}_e = 0 \quad (23)$$

- d) The reflected magnetic field:

$$\underline{H}_r = -\frac{\underline{E}_r}{\underline{Z}_0} = \frac{\underline{E}_e}{\underline{Z}_0} = \underline{H}_e \quad (24)$$

- e) The magnetic field transmitted in metal, at the boundary:

$$\underline{H}_i = \underline{H}_e + \underline{H}_r = 2\underline{H}_e \quad (25)$$

The conclusions yielded from the analysis of the numerical data yielded by the equations (21)-(25) are:

- The metallic surface reflects (practically in totality) the electric field component. This component does no longer penetrate the metal. On the metal surface a steady electric wave node is formed.
- A magnetic field amplified to the value $2\underline{H}_e$ penetrates the metal.

4. WAVE CROSSING FROM THE CONDUCTING METAL TO AIR

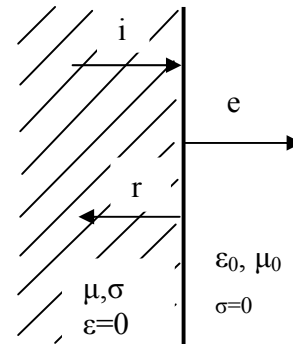


Figure 4: Plane wave exiting from the metal

The relations describing the electromagnetic state at the boundary between the metal and air are [3]:

- a) the phase relations:

$$\underline{E}_i + \underline{E}_r = \underline{E}_e \quad (26)$$

$$\underline{H}_i + \underline{H}_r = \underline{H}_e \quad (27)$$

- b) the relation for the propagation sense:

$$\underline{H}_r = -\frac{\underline{E}_r}{\underline{Z}_w} \quad (28)$$

The relation (26) can be written under the form:

$$\frac{\underline{E}_i}{\underline{Z}_w} - \frac{\underline{E}_r}{\underline{Z}_w} = \frac{\underline{E}_e}{\underline{Z}_0} \quad (29)$$

From the relations (26) and (27) one gets the expression for the electric field that leaves the metal (at the boundary) and passes to air:

$$\underline{E}_e = \frac{2\underline{Z}_0}{\underline{Z}_0 + \underline{Z}_w} \underline{E}_i = \underline{F}_2 \underline{E}_i \quad (30)$$

In this relation the refraction factor has the expression:

$$\underline{F}_2 = \frac{2\underline{Z}_0}{\underline{Z}_0 + \underline{Z}_w} \quad (31)$$

The reflected electric field is also obtained:

$$\underline{E}_r = \frac{\underline{Z}_0 - \underline{Z}_w}{\underline{Z}_0 + \underline{Z}_w} \underline{E}_i = \underline{R}_2 \underline{E}_i \quad (32)$$

with the following notation for the *reflection factor*:

$$\underline{R}_2 = \frac{\underline{Z}_0 - \underline{Z}_w}{\underline{Z}_0 + \underline{Z}_w} \quad (33)$$

The magnetic field transmitted at the boundary has the expression:

$$\underline{H}_e = \frac{\underline{E}_e}{\underline{Z}_0} \quad (34)$$

One can notice that the relations used for the calculation of the refraction and reflection factors \underline{F}_2 and \underline{R}_2 have the same structure as their counterparts \underline{F}_1 and \underline{R}_1 , but with a reversed role for the wave impedances \underline{Z}_0 and \underline{Z}_w .

A series of calculations were made in order to describe the electromagnetic state determined when a plane wave exists from a steel half-space toward air [3].

a) The reflection factor

$$\underline{R}_2 = \frac{\underline{Z}_0 / \underline{Z}_w - 1}{\underline{Z}_0 / \underline{Z}_w + 1} = \frac{377 / 7.695 \cdot 10^{-3} e^{j\pi/4} - 1}{377 / 7.695 \cdot 10^{-3} e^{j\pi/4} + 1} \approx 1 \quad (35)$$

b) The electric field reflected in air:

$$\underline{E}_r = \underline{R}_2 \underline{E}_i = \underline{E}_i \quad (36)$$

c) The electric field transmitted at the boundary, in air:

$$\underline{E}_e = \underline{F}_2 \underline{E}_i = (1 + \underline{R}_2) \underline{E}_i = 2 \underline{E}_i \quad (37)$$

d) The magnetic field reflected in air:

$$\underline{H}_r = -\frac{\underline{E}_r}{\underline{Z}_w} = -\frac{\underline{E}_i}{\underline{Z}_w} = -\underline{H}_i \quad (38)$$

e) The magnetic field transmitted at the boundary, in air:

$$\underline{H}_e = \underline{H}_i + \underline{H}_r = \underline{H}_i - \underline{H}_i = 0 \quad (39)$$

Considering the relations (35)... (39) one can see that, when the wave leaves the metal medium, the electric field is amplified to the value $2\underline{E}_i$ and the magnetic field is practically canceled.

5. THE BEHAVIOR OF DOUBLE LAYERED SHEETS AT THE IMPACT WITH THE ELECTROMAGNETIC RADIATION

A double layered shielded room is used for equipment with high performances. The first layer is made of a material with low μ_{ri} that does not reach the saturation state in the disturbing field and the second one, with a high μ_{ri} is no longer stressed during the saturation. The shield with low μ_{ri} must be placed toward the field source.

Figure 5 depicts the principle for the modeling of metallic sheet crossing by the plane electromagnetic wave. Refractions and reflections take place at both separation surfaces (air-metal, respectively metal-air).

The wave i_1 that comes out from the surface 1 is defined using the reflection factor \underline{R}_1 and respectively the refraction factor \underline{F}_1 .

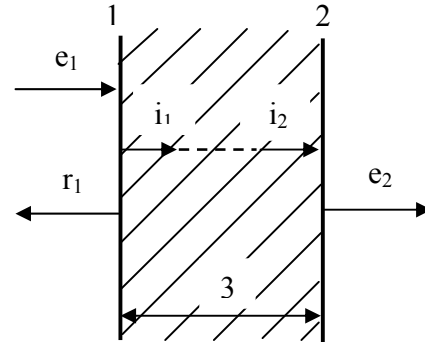


Figure 5: The metal sheet as barrier against electromagnetic radiations

Across the sheet width this wave is submitted to a damping process and a phase difference occurs too, being found as the wave i_2 along the surface 2 of the metal. The wave e_2 that comes out from the surface 2 is defined by the reflection factor \underline{R}_2 and respectively the refraction factor \underline{F}_2 [3], [6], [7], [8].

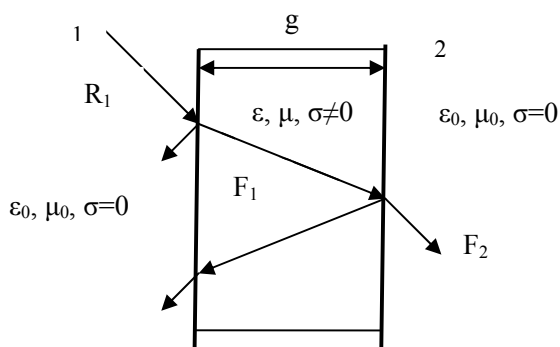


Figure 6: Multiple reflections and refractions

6. THE TESTING OF THE SHEETS MADE OF CuE AND STEEL

- Shielding with a *electrolytic copper* sheet (*CuE*)
- Shielding with a *steel* sheet (*Ol*)

In order to study the shielding effect one used a frequencies generator, two coils (for emission and receiving), a scope and a digital multimeter (fig.7).

The shields based on sheets were made of:

- electrolytic copper* – *CuE*
- Steel* – *Ol*.



Figure 7: Equipment used for tests

The waveforms for both coils were studied at a frequency of 90 kHz.

For the beginning the “receiver” coil was studied in the absence of shielding. The experimental tests performed in laboratory in the absence of any electromagnetic sources revealed a voltage drop across the terminals of the “transmitter” coil $U_{in} = 9.8$ V.

Corresponding to this voltage for the „receiver” coil the electric signal transposed into a voltage was $U_{off} = 4$ V (fig. 8). This value is lower than that from the „emission” coil

($U_{in} = 10$ V) due to the phenomenon known as magnetic field dispersion owing to the electromagnetic radiation. The distance between the coils is large enough so as to prevent the apparition of any electromagnetic induction (only the electromagnetic radiation is possible). In the second situation experiments were made with respect to the „receiver” coil during the shielding with the sheet made of *CuE*.

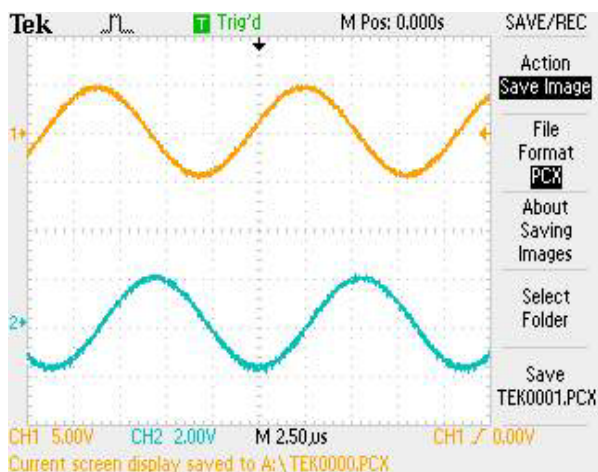
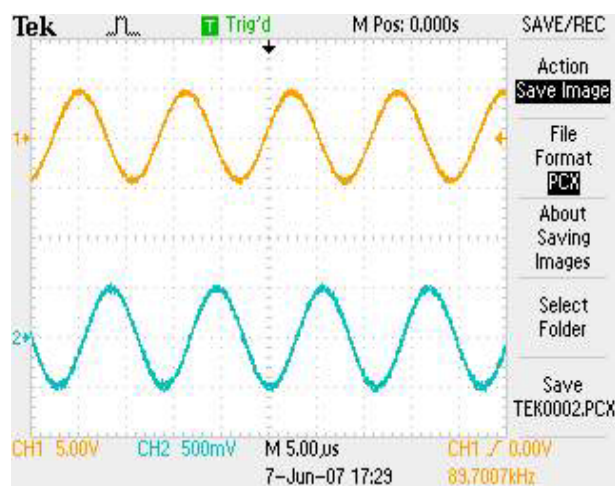


Figure 8: Waveforms for the „emission” coil (channel 1) and “receiver” coil (channel 2) in the absence of shielding

The measured voltage drop along the „emission” coil was $U_{in} = 9.8$ V and respectively the one along the „receiver” coil was $U_{off} = 1.6$ V (fig. 9). The sheet made of *CuE* performs a damping from 4 V to 1.6 V.

Figure 9: Waveforms for the „emission” coil (channel 1) and “receiver” coil (channel 2) when the shielding with a *CuE* sheet is performed

The third experiments concerned the „receiver” coil during the shielding with the sheet made of *steel*.

The measured voltage drop along the „emission” coil was $U_{in} = 9.8 \text{ V}$ and respectively the one along the „receiver” coil was $U_{off} = 1.3 \text{ V}$ (fig. 10).

The sheet made of steel performs a damping from 4 V to 1.3 V.

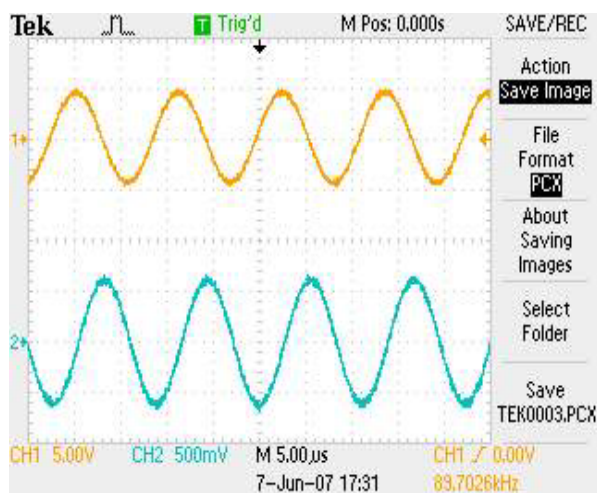


Figure 10: Waveforms for the „emission” coil (channel 1) and “receiver” coil (channel 2) when the shielding with a *steel* sheet is performed

7. CONCLUSIONS

The metallic sheet realized in the double-layer technology represents the main constructive element for the shielded room and for the room where the electromagnetic echo is absent [2], [9]. In principal the use of the metallic sheet has the following effects with respect to the electromagnetic waves penetration inside a shielded volume:

- It practically cancels the electric field inside the shielded volume, according to the relation (23), owing to the forming of an electric field node on the sheet external surface.
- It practically cancels the magnetic field inside the shielded volume, according to the relation (39).

In the constructions of high performances one uses a *double-layer* wall, as follows:

- sheets made of *CuE* in the outside part, in order to cancel the electric field;
- sheets made of *steel* in the inside part, in order to cancel the magnetic field.

The tested shields might be used for the urban electric driving systems in order to achieve the electromagnetic compatibility from the area where the power converters are placed.

Acknowledgments

This work was supported by ANCS Romania through the 4-th Program-Partnerships and under the Contract 71-145/2007.

References

- Schwab, Ad., „*Electromagnetic Compatibility* „, (in Romanian *Compatibilitate Electromagnetică*), Ed. Tehnică, Bucharest, 1996, pp. 157-201, 314-318;
- T. Tosaka, I. Nagano, S. Yagitani, “*Estimation of electric parameters for thin shielding sheets*”, Proceedings of IEEE International Symposium on Electromagnetic Compatibility, Chicago, USA, pp. 97-101, 2005;
- Hortopan, G., „*Electromagnetic Compatibility – Principals and Techniques*” (in Romanian *Principii și tehnici de Compatibilitate Electromagnetică*), Ed. Tehnică, București, 2005, pag. 81-140;
- T. Tosaka, I. Nagano, S. Yagitani, and Y. Yoshimura, “*Development of estimation system of relative permeability and conductivity of thin materials*,” proc of IEICEJ Trans. Commun., Vol. J87-B, No. 11, pp. 1943–1950, Nov. 2004
- Derik C. Love, Edward J. Rothwell “*A Mode-Matching Approach to Determine the Shielding Properties of a Doubly Periodic Array of Rectangular Apertures in a Thick Conducting Screen*” IEEE Transaction on Electromagnetic Compatibility, vol. 48, no.1, 2006, pp. 121-133;
- Mowete, I., Ogunsola, A., “*An Analytical Model for the Shielding Effectiveness of a Planar Multi-Layered Shield*”, proc. of EMC Europe 2006 Barcelona;
- F. Hang, L. Zhang, *Degeneration of shielding effectiveness of planar shields due to oblique incidence waves*, IEEE Transactions on Electromagnetic Compatibility, Volume 44(2), May 2002, pp. 353 – 363;
- M. Parise, M. S. Sarto, *Efficient formulation of higher-order boundary conditions for high frequency modeling of multilayer composite slab*, Proc. International Symposium on Electromagnetic Compatibility, August 18 – 20, 2003;
- D. Warkentin, A. Wang, W. Crunkhorn “*Shielded Enclosure Accuracy Improvements for MIL-STD-461E Radiated Emissions Measurements*”, Proceedings of IEEE International Symposium on Electromagnetic Compatibility, Chicago, USA, pp. 404-409, 2005.